Bollettino di Geofisica Teorica ed Applicata Vol. 41, n. 1, pp. 31-48; March 2000

Macroseismic attenuation relationships of Italian earthquakes for seismic hazard assessment purposes

L. Peruzza

CNR-GNDT at Istituto Nazionale di Oceanografia e di Geofisica Sperimentale, Trieste, Italy

(Received July 12, 1999; accepted January 27, 2000)

Abstract. In the frame of activities carried out in Italy for the seismic hazard assessment of the whole country, attenuation relationships were calibrated for macroseismic intensity. The attenuation curves follow the Grandori formulation, and were derived from the data sets of significant earthquakes; the results are presented and commented. Fifty-nine relationships, calibrated on more than 12 000 intensity observations, have been chosen to represent the regional patterns of intensity expected from some design earthquakes: this regionalization has seismic hazard purposes and has already been introduced into the national seismic hazard assessment. All the attenuation coefficients have to be used jointly with the earthquake catalogue, or linked to the present seismogenic zonation; both are prepared with the same hazard intent by the National Group for the Defence against Earthquakes. The reliability of these relationships is commented in relation to one mean curve derived from the same subset of macroseismic observations; even if the global residuals distribution does not favour the use of a multiple-law approach, a deeper analysis shows that the proposed regionalization gives a significantly better image of near-field damage, representing a first step towards a deterministic treatment of attenuation in probabilistic seismic hazard analyses.

1. Introduction

The use of macroseismic intensity as a ground shaking parameter started with the definition of the macroseismic scales themselves (see the latest, Grunthal, 1993); macroseismic attenuation relationships have been proposed since the beginning of this century (e.g.; Cancani, 1904). A very recent, and still debated, criticism is the one involving isoseismal maps, and the disuse of the practice of drawing them; the direct utilisation of point observations at the sites is becoming more

Corresponding author: L. Peruzza, CNR-GNDT at Istituto Nazionale di Oceanografia e di Geofisica Sperimentale, Borgo Grotta Gigante 42/c, 34010 Sgonico (TS), Italy; phone: +39 0402140244; fax: +39 040 2140266; e-mail: lperuzza@ogs.trieste.it

and more popular, and many authors now portray it as the best method of dealing with macroseismic data (e.g. Bakun and Wentworth, 1997; Musson, 1998)

Following this philosophy, this paper wants to present the database, and the macroseismic attenuation relationships obtained in the frame of the "Seismic hazard assessment of the national territory" Project of the Italian National Group for the Defence against Earthquakes (GNDT, see Corsanego et al., 1997). The macroseismic intensity relationships hereafter proposed have seismic hazard purposes, and three main requirements guided the analysis:

1. the coherence between the intensity data sets, the earthquake catalogue and related parameters, and the attenuation coefficients;
2. the need for the regionalization of attenuation that simply reproduces the damage distribution, adapted to the most significant or most dangerous earthquake experienced in the past;
3. the independence of the attenuation relationships from unavailable source parameters, or checkable for the majority of the strong events of the catalogue (e.g. depth, fault characteristics).

The above derived attenuation curves are strictly finalised for seismic hazard evaluation (Peruzza, 1996b; Slejko et al., 1998), and do not aim to describe either the physical properties of the crust, or the seismogenic processes involved. After failure of many investigations (e.g. Peruzza and Mucciarelli, 1997) to recognise significant differences between attenuation patterns for neighbouring zones in Italy, the attenuation characteristics derived from some design earthquakes have been selected as representative earthquakes for the seismogenic sources. They emphasise the contribution of one event with respect to others similarly originated inside a source, giving much more weight to the information derived from the strongest earthquakes. This choice represents an unusual application of deterministic attenuation to probabilistic seismic hazard analyses, and is an in-between flexible solution, nearer to the observed data with respect to the use of a mean relation for the whole territory, and not so complex as a physical simulation of the source. The task dealt with by representative earthquakes is a better reproduction of the effects of the most dangerous part of the macroseismic field: considering macroseismic data as an expression of source-path-site effects, where site conditions are averaged and smoothed by intensity assessment itself, the "single event" approach may better approximate near-field conditions. On the contrary, mean propagation properties necessarily enhance the behaviour of the majority of observations (as shown by soil acceleration attenuation relationships, see for instance Campbell, 1985) giving a better recovery of intermediate/far-field conditions. These are crucial aspects in seismic hazard analyses, which are partly overcome by this study.

2. How to derive attenuation curves from data points

The problem of the use of macroseismic intensities is particularly felt in Europe, and in countries with long written historical documentation (see for example Ambraseys, 1985; Stucchi, 1997).

In the frame of the activities sponsored by the GNDT, great efforts were made to investigate procedures for treating macroseismic data sets in order to obtain attenuation relationships. A long (and tedious) test phase has lead to some internal reports on the capability of attenuation rela-

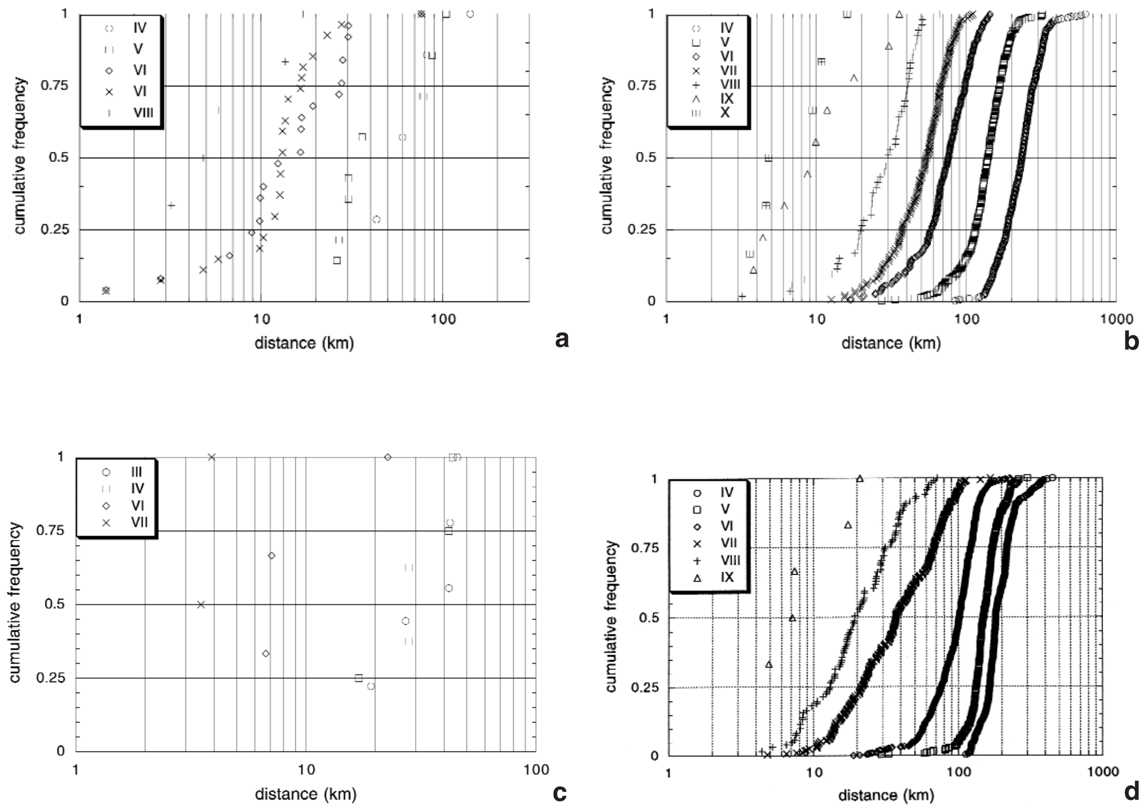

Fig. 1 - Cumulative curve samples of epicentral distances for some Italian earthquakes; a weight factor distinguishes certain from uncertain observations. The events are listed in Table 1: a) the oldest data set used in this analysis (earthquake of 1570); b) the most recent one (Southern Italy, 1980); c) the less documented earthquake (1917); d) the best documented one (1887).

tionships to reproduce observed damage (see Peruzza and Mucciarelli, 1997), and papers devoted to recognising homogeneous propagation properties, or the dependence of attenuation on the epicentral intensity (see Peruzza, 1995; 1996a; Cella et al., 1996). Finally, the relationship proposed by Grandori et al. (1987) as in Eq. (1)

$$I_0 - I_i = \frac{1}{\ln\psi}\ln\left[1+\frac{\psi-1}{\psi_0}\left(\frac{D_i}{D_0}-1\right)\right] \tag{1}$$

was adopted to model the damage distribution of representative earthquakes; in Eq. (1), I_0 indicates the epicentral intensity, I_i the intensity at the i^{th} site, D_i the distance of the site from the epicenter, and ψ, ψ_o and D_o are unknown coefficients.

Theoretically, in the Grandori formula, with the D_0 parameter, the inner part of the field has intensity values greater than I_o (i.e. negative intensity decay), an important peculiarity in the wide family of intensity attenuation relationships. The common practice cuts the curve with a flat step

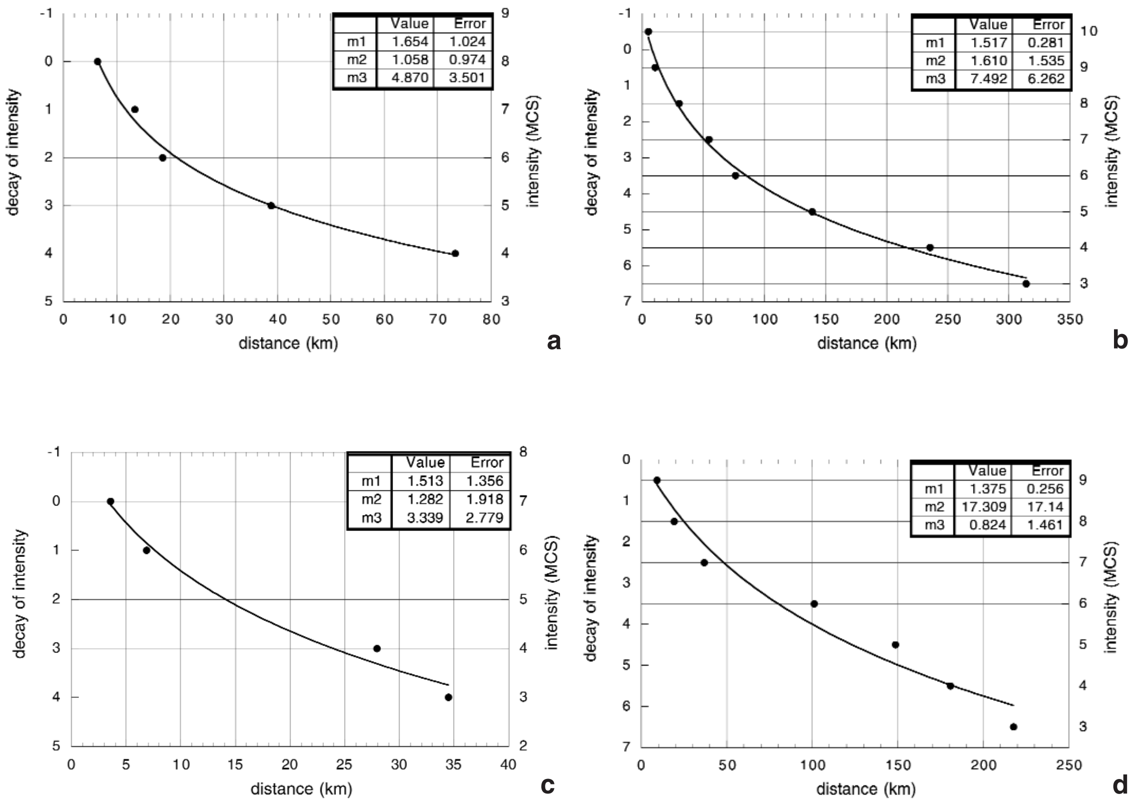

Fig. 2 - Curve fitting of Grandori Eq.(1) using the 50% sample distance of Fig. 1; a) 1570 earthquake; b) 1980 earthquake; c) 1917 earthquake; d) 1887 earthquake. Non-linear least squares method is used to derive the unknown coefficients, respectively m1, m2 and m3 correspond to ψ, ψ_O and D_O.

of zero-decay, for distances smaller than D_o to avoid numerical instabilities; it intends to model an somehow circular extended source; an approximation nearer to reality than the point source model. The formulation with three coefficients makes the relation very flexible, even if quite unstable; the formula may simulate a logarithmic-shaped curve, but also the less frequent conditions of linear decay of intensity with distance, and even an unusual increase of the decay rate. The authors (Grandori et al., 1987; 1988) calibrated the unknown coefficients using mean isoseismal distances: in addition they proposed the parameter Φ that makes the D_o coefficient dependent on the epicentral intensity I_o. The application hereinafter proposed is intended to calibrate the ψ, ψ_o and D_o coefficients from the data points directly: it has the advantage of being completely transparent and reproducible. As concerns coefficient Φ, *I* discarded the I_o dependance as not supported by the data (see e.g. Peruzza, 1996a).

The Grandori unknown coefficients are obtained from the macroseismic data set following four steps:

- the first step is to compute the distance of each site with the observed intensity from the epicentre reported in the earthquake catalogue;

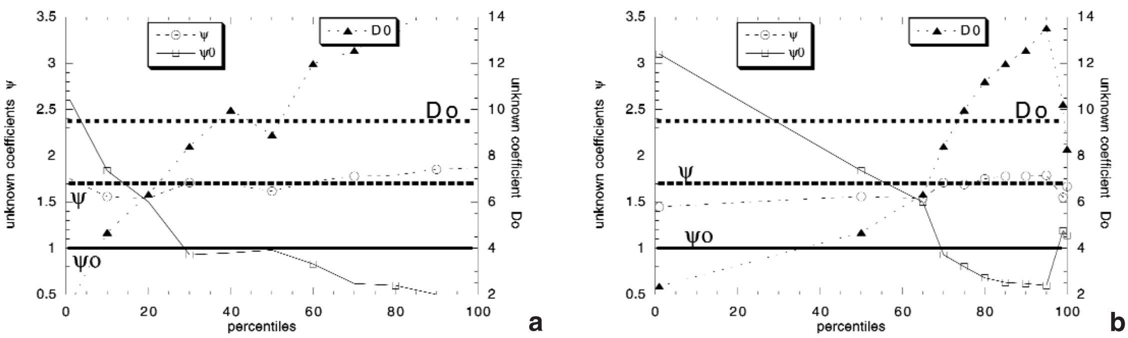

Fig. 3 - Synthetic test of attenuation coefficients determination as a function of the percentile threshold used: description in the text; a) using rounding algorithm; b) using truncation.

- the second, is to construct the sample cumulative curve of distances corresponding to the same macroseismic degree (Fig. 1); uncertain intensities (by definition given using double intensity values, or half degree, not defined by the macroseismic scale) are split into the relevant classes using a weight factor given by:

$$w_{obs} = \frac{1}{\left(I_{\max} - I_{\min}\right) + 1} \tag{2}$$

- the third is to select the empirical sample percentiles (distances expected not to be exceeded at a given probability level) for each intensity class, associated to its proper intensity decay. The distance corresponding to the 50% percentile is computed here, but only if the intensity class has at least three samples;
- the fourth is to apply a nonlinear least squares method to the couples of distance-intensity decay (Fig. 2), in order to derive the unknown coefficients of Eq. (1).

The methodology is widely presented and commented in Peruzza (1995; 1996a). The application presented uses empirical samples and does not superimpose probabilistic models onto the data (e.g. lognormal in the previously quoted works; Weibull and Gamma in Cella et al., 1996); probability distribution functions have been abandoned to avoid a priori assumptions on the populations of intensity observations.

The choice of a 50% fractile distance is consistent with the use of an ordinary rounding algorithm of real into integer conversion, to transform the estimate given by the curve in eqn.(1) into the predicted intensity at a given site. The synthetic test of Fig. 3 illustrates the convergence of the unknown parameters to the “true” value, as a function of the percentile threshold selected. Using the site locations of a recent earthquake (1980 Irpinia earthquake, with more than 1100 macroseismic observations; Postpischl et al., 1985), I computed the intensities expected at the sites, given some arbitrary Grandori coefficients (ψ, ψ_o and D_o, represented by horizontal lines in Fig. 3). Then I perturbated the computed intensities randomly, for a maximum amount of 0.5 degree; finally, I transformed the real expected intensities into integer values using a rounding algorithm (Fig. 3a) and truncation (Fig. 3b), as is frequently done by people handling intensity

Table 1 - Earthquakes selected for the calibration of attenuation relationships devoted to seismic hazard assessment: see the text. SZ field refers to the seismogenic zonation redrawn in Fig. 4; fields from N to Nip derive from the parametric catalogue (see Camassi and Stucchi, 1996): epicentral intensity and maximum intensity (respectively I_o and I_x) are expressed multiplied by 10, following the catalogue compilers habit. Max I_o field indicates the year and epicentral intensity of the strongest event in the source, if it differs from the selected one. Min I field indicates the lower threshold of intensity used. NTsam field indicates the number of samples that derive from splitting of uncertain intensity data. The last three fields report the values of the Grandori coefficients obtained.

SZ	N	Rt	Os	Date	Ix	Io	lat	lon	Nip	Max Io	Min I	N T sam	ψ	$ψ_0$	D_0
03	69	RIB82	4P	1895 04 14	90	85	46.100	14.500	953	*	≥ III	1299	1.552	1.853	7.369
04	177	GDTSP	6U	1976 05 06	95	95	46.232	13.066	740	*	≥ III	1064	1.963	0.569	8.988
05	192	BAA86	4P	1936 10 18	90	90	46.067	12.367	263	1873/95	≥ III	312	2.609	0.170	9.716
06	204	ENL85	1R	1695 02 25	90	95	45.875	11.915	73	*	≥ IV	103	1.446	19.698	0.666
07	242	ENL85	1R	1891 06 07	80	80	45.567	11.150	262	1117/95	≥ III	334	2.269	1.346	3.324
08	270	CFT95	3P	1901 10 30	80	80	45.583	10.373	170	1222/85	≥ III	213	1.498	1.753	6.230
09	289	BRA85	5P	1802 05 12	80	80	45.383	9.833	49	*	≥ IV	61	2.392	1.127	4.685
16	399	ENL85	1R	1892 03 05	75	70	45.617	7.800	63	*	≥ III	72	1.164	1.568	4.344
19	423	ENL85	1R	1808 04 02	80	80	44.817	7.283	65	*	≥ III	72	2.043	1.002	4.636
21	463	CFT95	3P	1959 04 05	75	70	44.497	6.735	60	*	≥ V	69	2.608	1.012	9.348
22	479	CFT95	3P	1887 02 23	100	95	43.883	8.100	1367	*	≥ III	1768	1.375	17.309	0.824
26	523	ENL85	1R	1828 10 09	80	75	44.816	9.097	87	*	≥ III	123	1.943	0.865	11.148
28	563	FEA85	5P	1920 09 07	100	95	44.200	10.200	454	*	≥ III	569	1.505	1.684	4.429
29	585	MAM83	2U	1904 06 10	80	75	44.250	10.750	48	*	≥ III	60	0.918	7.416	1.766
30	641	ENL85	1R	1971 07 15	80	75	44.783	10.383	224	1501/85	≥ III	279	1.491	1.213	9.820
31	670	CAA96	6U	1846 08 14	90	85	43.500	10.500	83	*	≥ III	114	1.602	0.854	3.593
33	739	MAM83	2U	1904 11 17	70	70	43.950	10.817	89	1293/80	≥ III	105	1.577	6.552	1.413
35	774	CAM94	6P	1929 04 20	75	70	44.450	11.133	105	1869/75	≥ III	131	2.051	2.365	3.806
36	788	FEP85	5P	1919 06 29	90	90	43.950	11.483	149	*	≥ III	180	1.477	2.988	2.181
37	816	POS90	6U	1918 11 10	80	80	43.950	11.867	93	1661/90	≥ III	110	1.238	2.679	3.786
38	840	POS90	6U	1781 04 04	90	90	44.233	11.750	74	*	≥ III	97	2.443	0.518	3.588
39	868	ENL85	1R	1570 11 17	80	80	44.817	11.650	40	*	≥ III	56	1.654	1.058	4.870
40	896	POS90	6U	1911 02 19	75	75	44.100	12.067	120	*	≥ III	141	1.528	0.960	8.308
41	918	ENL95	1U	1919 09 10	80	80	42.767	11.783	48	*	≥ III	64	1.268	1.784	3.447
42	943	ENL95	1U	1969 07 02	70	70	42.167	12.017	67	*	≥ III	72	1.003	2.293	2.694
43	954	MOL81	2U	1806 08 26	80	75	41.700	12.717	25	*	≥ III	29	1.786	1.448	6.220
44	990	DOM80	2U	1917 05 12	80	70	42.583	12.617	18	1901/75	≥ III	20	1.513	1.282	3.339
45	1046	CAA96	6U	1917 04 26	95	90	43.483	12.117	106	*	≥ III	182	1.454	2.560	1.745
46	1075	MON87	6U	1781 06 03	100	95	43.583	12.500	143	*	≥ III	224	1.539	0.855	5.565
47	1186	SPA81	5P	1979 09 19	85	80	42.717	12.950	235	1703/100	≥ III	273	1.299	1.116	11.271
48	1218	MOM92	2P	1930 10 30	85	85	43.633	13.333	220	*	≥ III	282	1.764	0.593	10.649
50	1290	DOM80	2U	1922 12 29	70	70	41.717	13.633	99	1349/100	≥ III	118	1.289	0.880	14.330
51	1308	MOA96	4U	1915 01 13	110	110	42.028	13.489	949	*	≥ III	1430	1.439	0.497	11.379
53	1378	RAA85	5P	1943 10 03	90	85	42.917	13.617	86	*	≥ III	99	1.835	0.408	9.616
54	1389	FRA88	2P	1960 01 11	75	70	41.267	13.983	18	*	≥ III	23	1.233	1.379	2.434
55	1409	MAA92	2U	1933 09 26	90	90	42.100	14.100	297	1706/95	≥ III	333	1.544	0.537	9.897
56	1434	CFT95	3P	1883 07 28	100	90	40.750	13.886	25	*	≥ III	32	1.782	0.378	2.027
57	1441	GDTSP	6U	1903 05 04	75	70	41.033	14.533	27	*	≥ III	40	1.193	3.163	0.806
58	1457	POA88	4P	1805 07 26	110	100	41.500	14.533	208	1688/110	≥ III	217	1.628	0.705	9.556
59	1476	ENL85	1R	1627 07 30	110	105	41.733	15.267	45	*	≥ V	76	1.412	0.892	8.689
62	1543	SPA85E	5P	1930 07 23	100	100	41.050	15.300	284	*	≥ III	323	1.374	1.484	6.630
63	1587	POA85	5P	1980 11 23	100	95	40.800	15.267	1137	1857/105	≥ III	1249	1.517	1.610	7.492
65	1595	ENL85	1R	1836 04 25	100	95	39.567	16.700	37	*	≥ V	45	1.273	3.515	2.169
66	1604	ENL85	1R	1638 03 27	110	110	39.083	16.283	205	*	≥ VI	298	1.535	0.504	10.299
67	1632	ENL85	1R	1832 03 08	100	95	39.050	16.917	52	*	≥ V	74	1.690	0.448	10.318
68	1644	ENL85	1R	1783 03 28	110	100	38.800	16.467	317	*	≥ V	454	1.517	0.833	9.536
69	1672	CFT95	3P	1905 09 08	105	110	38.754	16.026	733	*	≥ III	994	1.314	10.298	0.975
70	1692	CFT95	3P	1947 05 11	90	85	38.712	16.581	161	*	≥ III	230	1.282	1.037	9.007
71	1728	BAA80	5P	1908 12 28	110	110	38.133	15.667	182	*	≥ III	222	1.586	0.683	9.254
72	1752	CFT95	3P	1907 10 23	90	85	38.155	16.024	264	*	≥ III	374	2.345	0.102	13.695
73	1803	PAI85	5P	1914 05 08	90	85	37.650	15.150	47	1911/95	≥ V	58	2.162	0.373	2.123
74	1878	BAA80	5P	1978 04 15	80	85	38.150	14.983	280	*	≥ III	326	1.388	1.063	8.327
75	1896	BAA80	5P	1967 10 31	80	80	37.850	14.367	56	*	≥ III	91	1.569	0.573	9.869
76	1912	BAA80	5P	1940 01 15	80	75	38.033	13.433	25	1823/85	≥ III	30	1.277	2.081	3.905
77	1925	COM85	5P	1968 01 15	100	95	37.750	12.967	159	*	≥ III	206	1.656	0.871	7.404
79	1951	CFT95	3P	1693 01 11	110	105	37.443	15.192	179	*	≥ III	243	1.219	0.572	25.277
80	1965	ENL85	1R	1743 02 20	90	105	39.667	19.000	63	*	≥ IV	84	1.415	22.866	1.323
bkb	2113	GDTSP	6U	1951 05 15	60	65	45.300	9.617	121	*	≥ III	125	1.070	3.534	11.180
bkd	2116	GDTSP	6U	1956 01 09	70	65	40.567	16.383	41	*	≥ III	49	1.255	3.971	3.151

data. The data sets are then treated following the four steps described previously, to check which percentile threshold drives back to the original ψ, ψ_o and D_o, when random noise, and systematic bias (real into integer conversion) are applied to the synthetic data. The graphs show the variation of the Grandori coefficients obtained by the fitting, as a function of the fractile threshold chosen. The coefficients converge towards the initial values near to the 50% threshold using rounding (Fig. 3a) and near to 100% using truncation (Fig. 3b). Therefore, the coefficients obtained in this paper must be used, jointly, with ordinary rounding algorithms.

In the approach proposed here, intermediate degrees are not treated as separate classes; an intensity assessment reported as VI-VII is split into two samples of the same coordinates, and half weight, both in the classes VI and VII; observations not consistent with the macroseismic scale are therefore counted on both sides equally.

The method proposed has the advantage of being completely transparent and reproducible. It establishes, in practice, some rules for attenuation curve fitting using macroseismic data: it can be applied to any attenuation model, as long as one accepts the fact that the coefficients obtained are the result of a minimization on selected distance-intensity decay couples; they are, therefore, dependent on the epicentral coordinates and intensity. This model represents a small contribution for the formalization of macroseismic intensity treatment, a problem often disregarded by the seismological community.

3. Data analysis

More than one hundred earthquakes were treated following the methodology mentioned above. Most of them were processed many times, using different sources of the macroseismic data sets, or revised versions.

Table 1 contains the main information regarding the selected events. In particular, the first ten fields were taken from the earthquake catalogue (Camassi and Stucchi, 1996), while the last ones are the result of this elaboration. The final data sets, from which the epicentral parameters of the catalogue were derived, are available at the GNDT web site (Monachesi and Stucchi, 1997) or reported in Boschi et al. (1997). I reported all those fields to stress again that different epicentral parameters (latitude, longitude, and epicentral intensity, i.e. a different parametric catalogue) imply a new parametrization of the attenuation coefficients, even if it refers to the same data sets.

The final attenuation coefficients were associated to the seismogenic zonation proposed by GNDT (Scandone, 1997); in Fig. 4, the grey areas indicate sources that have their own attenuation relationship for macroseismic intensity. The one-source/one-attenuation-relationship was the ultimate solution, after many investigations failed to find homogeneous propagation properties of macroseismic intensity. In fact, inside many seismogenic sources (SZ) - assumed homogeneous at their interior in terms of expected earthquake characteristics by the zonation, and similarly considered homogeneous in the assumptions of the seismic hazard approach (Cornell, 1968; Bender and Perkins, 1987) - earthquakes often exhibit different propagation properties. As we are not able to ascertain either the source, path and site effects, or the bias due to insufficient

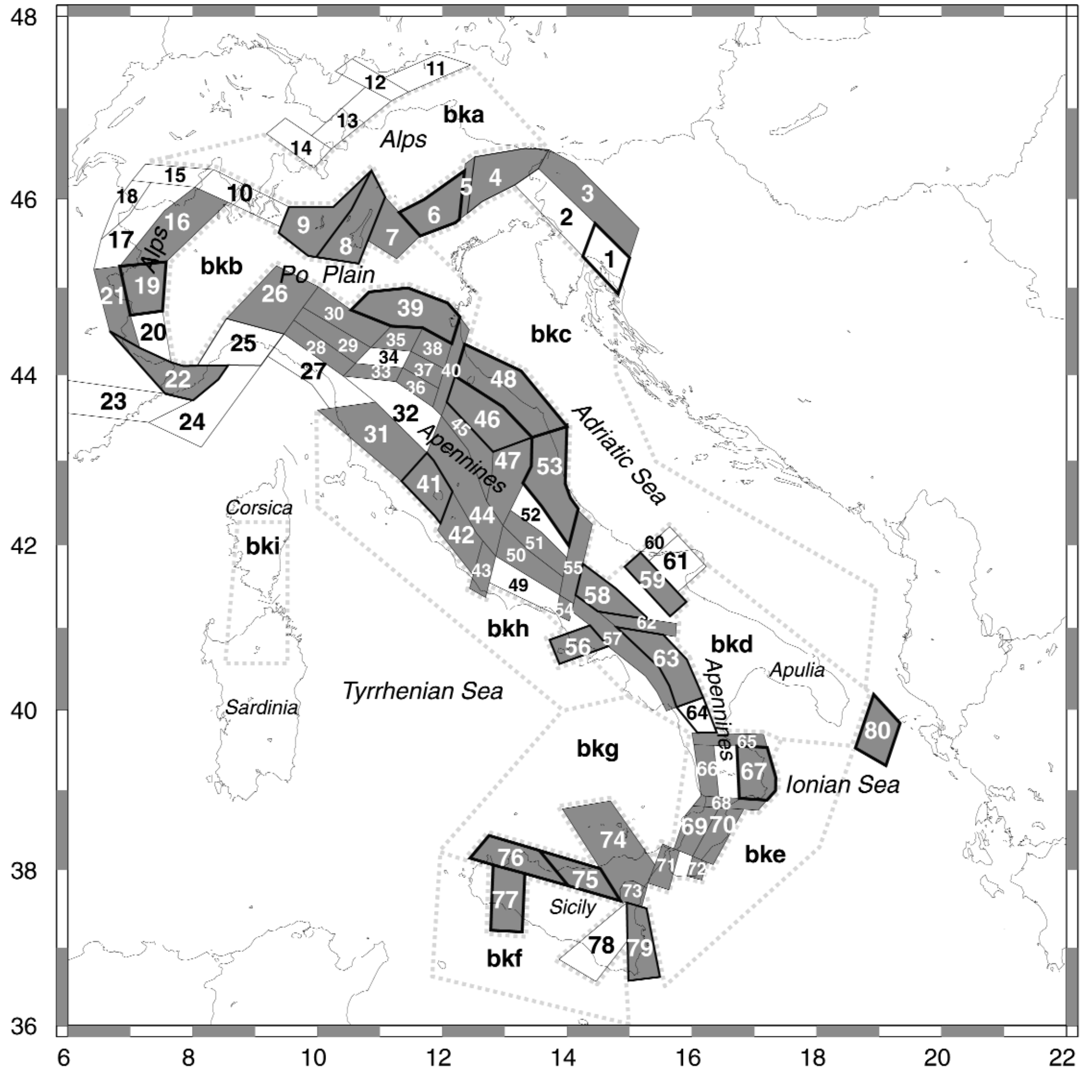

Fig. 4 - Map of the seismogenic sources used in the seismic hazard assessment (redrawn from Slejko et al., 1998); grey areas have their own proper macroseismic attenuation relationship.

spatial sampling, or the influence related to different data set compilers, just one event has been selected as "representative earthquakes"; usually it is the strongest event occurring in the SZ. In Table 1, an asterisk in the "Max I_o" column indicates the SZs where the selected earthquake is the maximum one experienced in the past: for the other cases, chosen after a quality evaluation of the data set, the Table 1 reports the year and I_o of the last maximum event of the SZ.

In Table 1, the "NTsam" column indicates the total number of samples which derives from the total number of points having macroseismic intensity (Nip), after uncertain data have been split into different intensity classes. The more the "NTsam" differs from the "Nip" value, the more the data set is characterised by an uncertain evaluation of the intensity degree; on average, data sets have less than 30% uncertain data points.

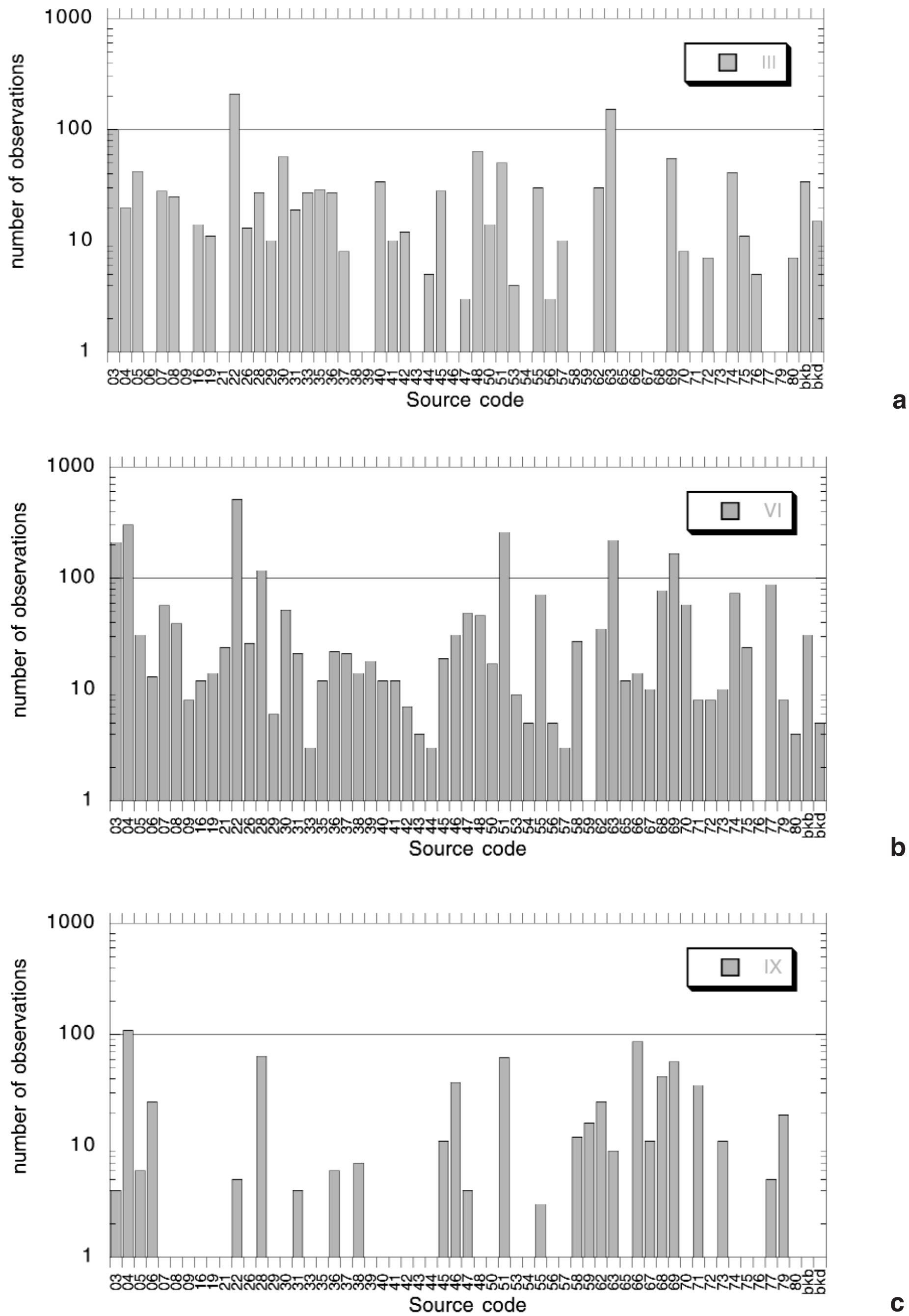

Fig. 5 - Data samples used for each SZ: a) intensity class III MCS; b) VI MCS; c) IX MCS. The number of observations reported on Y-axis is weighted using Eq. (2).

Fig. 5 shows the number (weighted according to uncertainties) of observations used in three different intensity classes for the selected earthquakes: the SZ code of Table 1 is reported in the X-axis; the intensity classes with less than three intensity data points are empty. Fig. 2 shows

Table 2 - Earthquakes rejected in this analysis: on the left, the events which permitted the calibration of the Grandori relationship; on the right, those that did not; see the text.

SZ	Date			I_o	ψ	ψ_0	D_0	SZ	Date		
4	1511	03	26	90	4.77	0.26	17.3	**9**	1894	11	27
4	1928	03	27	85	1.96	1.04	3.3	**15**	1855	07	25
6	1695	02	25	100	2.27	0.65	6.5	**26**	1873	09	17
38	1688	04	11	90	0.56	3.90	3.4	**26**	1972	01	18
41	1971	02	06	75	1.14	12.26	0.6	**27**	1913	12	07
43	1919	10	22	70	1.01	8.25	2.8	**27**	1945	06	29
43	1927	12	26	75	1.47	4.01	1.1	**31**	1909	08	25
46	1741	04	24	90	1.77	0.76	9.8	**32**	1812	09	11
47	1898	06	27	75	1.56	2.04	4.0	**35**	1929	07	28
50	1654	07	23	95	5.28	0.10	9.4	**47**	1898	08	28
58	1962	08	21	90	1.17	1.40	9.6	**48**	1690	12	22
67	1638	06	09	95	0.18	1.74	14.8	**48**	1786	12	25
73	1818	02	20	90	1.39	4.61	2.5	**50**	1349	09	09
74	1926	08	17	75	1.29	28.50	0.7	**52**	1639	10	07
79	1693	01	11	110	0.95	0.83	18.7	**53**	1950	09	05
bki	1948	11	13	60	28.9	0.09	15.8	**56**	1828	02	02
								59	1731	03	20
								62	1851	08	14
								63	1857	12	16
								69	1783	02	05

some examples of curve fitting (events reported in Fig. 1); the problem of curve reliability will be described in the following.

Finally, Table 2 reports other earthquakes submitted to the same treatment during the analysis, and then discarded. Some of them (left side of the table) led to attenuation coefficients that may be used in deterministic applications, but were abandoned for the probabilistic seismic hazard assessment as they did not fullfill the criteria of representative earthquakes (strongest event, with highest data set quality); others (on the right) are poorly documented earthquakes, that did not reach the minimal conditions for the curve fitting (three intensity classes, each with at least three samples), or failed to reach the convergence conditions. Unique exception: the earthquake of 1693, belonging to SZ 79, that is reported both in Tables 1 and 2. The coefficients in Table 2 derive from the study by Barbano (1985) while those in Table 1 come from the data set reported in Boschi et al. (1995). The second one was preferred in the last version of the earthquake catalogue, nevertheless the first one is reported too, since it was used in the hazard computation (Peruzza, 1996b; Slejko et al., 1998). If we compare the coefficients of the Grandori relationships presented in Peruzza (1996b) to the present ones, we may note some differences: some slightly different epicentral parameters have been introduced in the last version of the catalogue, as well as minor changes in the data sets with respect to those used in 1996; in addition, this analysis uses all the available intensity classes, while the preliminary study (Peruzza, 1996b) was focused on intensity classes greater than IV, a fact that introduces some problems in controlling the attenuation curve queues. It has to be stressed, anyway, that even if the coefficients

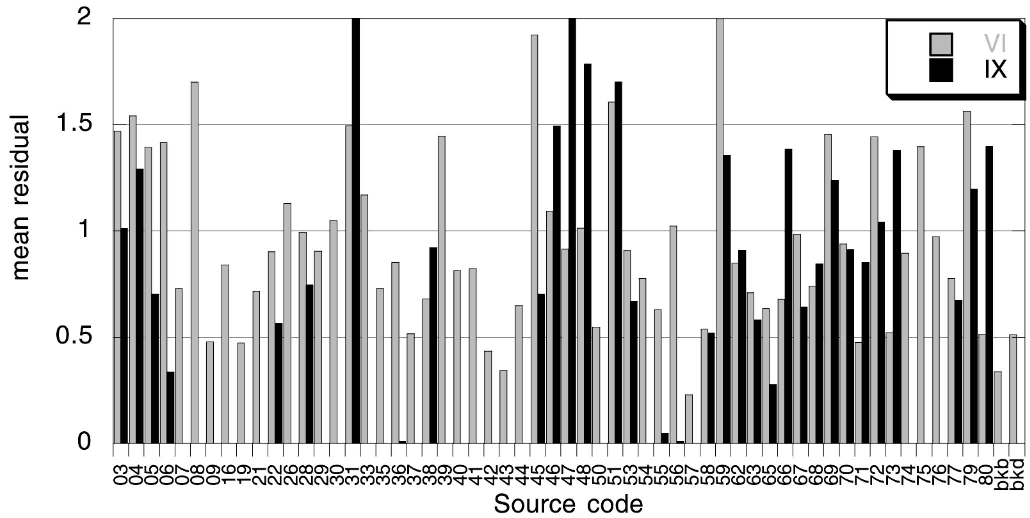

Fig. 6 - Mean residual of two intensity classes on each data set; MR is obtained by Eq. (4).

of the two studies are sometimes quite different, the curves are always very similar, and the only notable difference on a seismic hazard map is related to the newly selected data set of SZ 79.

The white SZs in Fig. 4 were not characterized by their own attenuation coefficients: the related seismicity, and available data sets did not reach the criteria for consideration as representative earthquakes. These sources have been treated in the final seismic hazard assessment of Italy (Slejko et al., 1998) using a mean attenuation relationship derived by Mucciarelli (see Peruzza and Mucciarelli, 1997) from the same selected earthquakes reported in Table 1. Its formula is (following Magri et al., 1994; Berardi et al., 1994):

$$I_0 - I_i = \alpha + \beta \sqrt[3]{D_i} \tag{3}$$

where α=-0.769 and β=1.015, I_o, I_i and D_i have the same meaning of Eq. (1). It will be referred to in the following as the mean CRAM model, and used for comparison.

4. Reliability

The reliability of the attenuation relationships previously obtained cannot simply be expressed in terms of statistical error of the curve fitting, because the use of the 50% fractile distance artificially reduces the variance of observed data. This is the reason why the statistical errors obtained in the minimization procedure for the unknown coefficients (see the legend of each frame, in Fig. 2) are not reported in Table 1.

Therefore, the quality of the attenuation curves has been evaluated in terms of residuals, with respect to the observations. The mean residual is defined as Eq. (4)

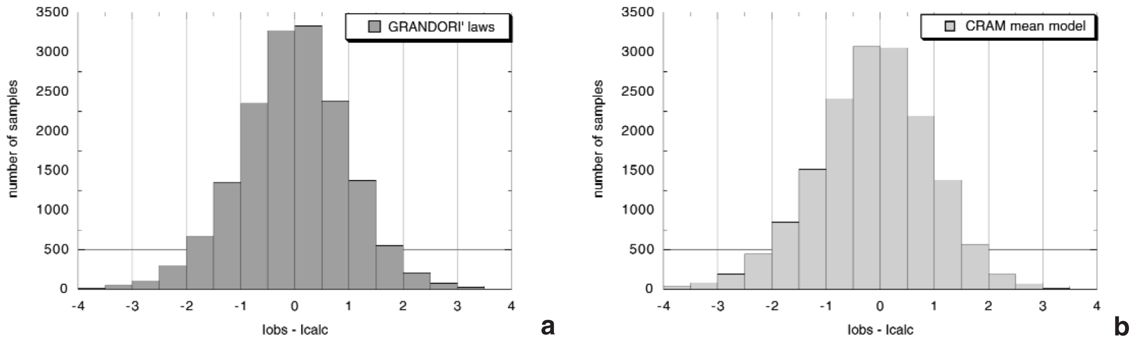

Fig. 7 - Distribution of the residual ($I_{observed} - I_{calculated}$) for the whole selected data sets; a) according to the multiple Grandori coefficients; b) according to the mean CRAM model.

$$MR = \sum_{i=1}^{N} \left| I_{obs_i} - I_{cal_i} \right| \Big/ \sum_{i=1}^{N} w_i \qquad (4)$$

where w_i indicates the weight given to each observation. As the modulus of the residual is considered, MR represents the most cautious error evaluation. MR can be computed on the whole data, or on each intensity class.

Fig. 6 plots the mean residuals of the data sets for two intensity classes (VI and IX MCS) of particular interest; they are selected as in the statistical meaning of macroseismic scale definition (Console e Gasparini, 1977), these classes may represent the first damage, and collapse levels for ordinary buildings. The MR oscillates around the value of 0.8, for both intensity classes; the fluctuation is wider for the highest shaking, not present in all the earthquakes, and is certainly based on a lower number of observations (see in Figs. 5b and 5c). Three cases exhibit an MR greater than 2: SZ 31 and SZ 47, with the MR equal to 2.3 for intensity IX, and SZ 59 with 3.3 for intensity VI. The highest MR values always refer to very few data points, where both the 50% fractile distance looses its meaning, and the local high residuals (for example due to site response) cannot be smoothed by other observations (small Σw_i in Eq. (4)). An exemplary case is represented by intensity class VI of SZ 59; the selected data set presents only two localities with those effects (Chieti, V-VI; Torre Santa Susanna, VI-VII): the fractile distance of class VI cannot be computed, for insufficient samples (see Fig. 5b), and the curve fitting is controlled by the adjacent classes V and VII; the intensity computed at the sites, using the coefficients of Table 1 is respectively 5.3 (Chieti) and 3.4 (Torre Santa Susanna); in the first case, the predicted value is perfectly coherent with the observation, while in the second the observed data is much higher, probably the result of an anomalous amplification. The uncertainty in the intensity assessment leads to a half weight for each observation, so that the MR for class VI reaches the value of 3.3; other observations in the same class would have reduced the impact of one high local residual.

The distribution of the residuals ($I_{observed} - I_{calculated}$) on the entire population of intensity points (more than 12 000 observations which became more than 16 000 weighted samples for

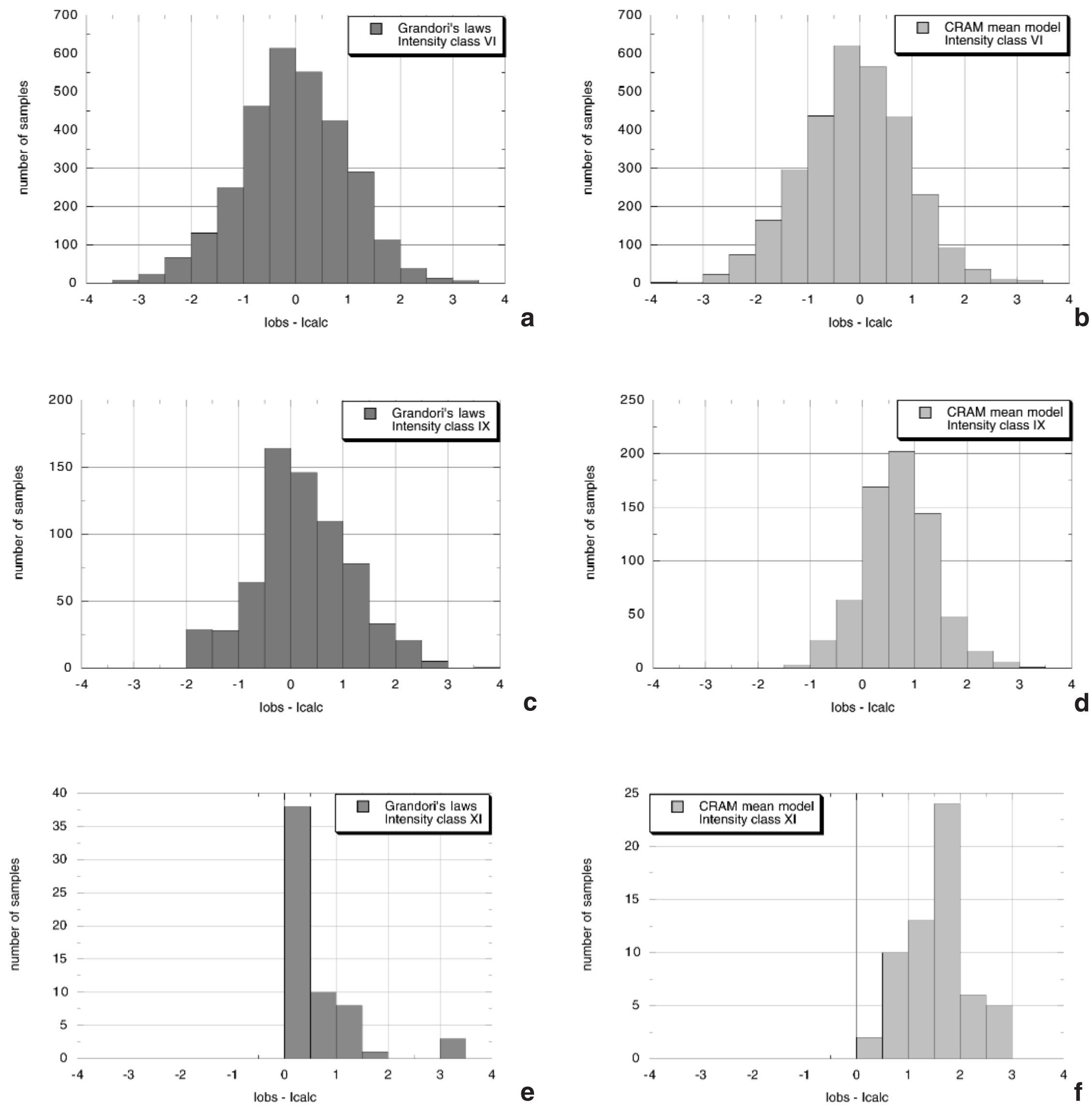

Fig. 8 - Distribution of the residual for given intensity classes according to multiple Grandori coefficients (a, c, e) and mean CRAM model (b, d, f); intensity classes VI, IX, and XI are shown.

"uncertainties" splitting) is given in Fig. 7a; the residuals with the CRAM average model have been computed too (Fig. 7b). Comparing the global residuals distribution, one may argue that the use of multiple attenuation coefficients does not significantly improve the macroseismic predicted values, with respect to the use of one single mean relationship. On the contrary, the distribution of residuals plotted for each intensity class (Fig. 8 for classes VI, IX and XI) supports the multiple-laws choice; the use of different coefficients, combined with the peculiar Grandori formulation with zero-decay for distances smaller than D_0, simulates the near-field behaviour better as the residuals of the higher intensity classes (Figs. 8c, e) remain centred on the zero value;

Table 3 - Statistical analysis of the residuals.

Variable	Points	Mean	Median	RMS	Std Deviation	Variance	Skewness	Kurtosis
GRAND III	1311	-0.257	-0.280	0.910	0.874	0.764	0.561	4.280
CRAM III	*1311*	*-0.859*	*-0.916*	*1.393*	*1.097*	*1.204*	*0.038*	*-0.121*
GRAND IV	2535	-0.046	-0.007	0.993	0.992	0.985	-0.257	0.574
CRAM IV	*2535*	*-0.385*	*-0.435*	*1.047*	*0.974*	*0.949*	*0.082*	*0.279*
GRAND V	2718	0.043	0.127	1.020	1.019	1.040	-0.310	0.611
CRAM V	*2718*	*-0.184*	*-0.112*	*1.062*	*1.046*	*1.095*	*-0.035*	*0.327*
GRAND VI	3004	-0.053	-0.054	1.038	1.037	1.076	-0.207	0.564
CRAM VI	*3004*	*-0.116*	*-0.090*	*1.018*	*1.012*	*1.024*	*-0.049*	*0.196*
GRAND VII	3099	-0.101	-0.037	1.027	1.022	1.046	0.602	9.487
CRAM VII	*3099*	*-0.004*	*0.008*	*0.872*	*0.872*	*0.761*	*0.108*	*0.237*
GRAND VIII	1974	0.075	0.077	0.991	0.989	0.978	0.143	2.865
CRAM VIII	*1974*	*0.330*	*0.294*	*0.852*	*0.786*	*0.618*	*0.114*	*0.090*
GRAND IX	679	0.179	0.136	0.979	0.963	0.928	0.111	0.135
CRAM IX	*679*	*0.691*	*0.685*	*0.970*	*0.680*	*0.463*	*0.160*	*0.369*
GRAND X	281	0.229	0.057	0.960	0.934	0.872	0.787	0.351
CRAM X	*281*	*1.124*	*1.183*	*1.274*	*0.600*	*0.360*	*-0.134*	*0.213*
GRAND XI	60	0.482	0.084	0.907	0.774	0.600	2.316	5.451
CRAM XI	*60*	*1.531*	*1.570*	*1.636*	*0.582*	*0.338*	*0.127*	*-0.086*

the mean CRAM relationship underestimates systematically the intensities near the epicentre (Figs. 8d, f), while it shows an adequate approximation in the far field (compare Figs. 8a and 8b, referred to intensity VI). The complete statistical analysis of the residuals, intensity class by intensity class, is reported in Table 3. A proper approach to attenuation reliability should consider both local soil conditions, and a quality factor of each macroseismic data points: this is one of the aspects that needs future investigation. Nowadays, the standard deviations of each intensity class for each representative earthquake have no practical use; a σ of about 0.9 degree may be considered a reasonable average of all the MRs obtained, and can be used to estimate the attenuation uncertainty when the relationships proposed here are entered into seismic hazard assess-ment; this value is comparable with the intrinsic uncertainties of intensity estimates.

5. Results

Fig. 9 shows the attenuation curves obtained for each SZ (the grey areas of Fig. 4): the mean attenuation obtained with the CRAM model on the whole data set is reported too. They are commented on by geographical criteria, starting from the north.

In the Central-Eastern Alps (Fig. 9a), all the curves lie in a range of about one degree with respect to the mean attenuation for distances greater than 20 km. In the near field - an observation valid for all the graphs - the CRAM formulation underestimates the expected intensities with respect to the Grandori ones. Nearly the same considerations, referring to the Western Alps and Northern Tuscany, are valid for Fig. 9b; here, two SZs (16, and 29) present a rapid quasi-linear

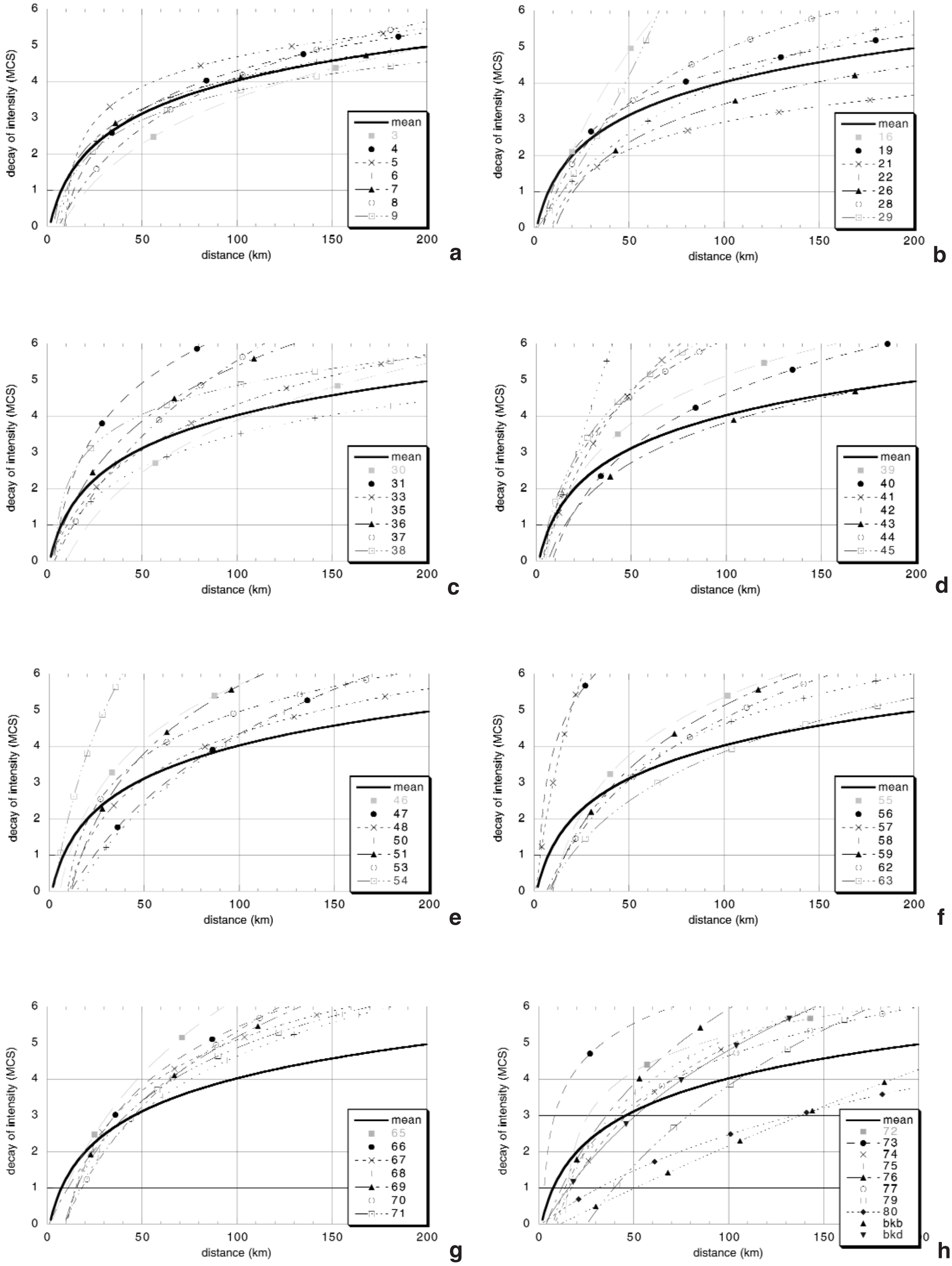

Fig. 9 - Representation of the attenuation relationships obtained for seismic hazard purposes; the curves are shown according to geographical criteria: a) Central-Eastern Alps; b) Western Alps, Tuscany; c) Northern Apennines; d) Central Apennines; e) Central Apennines; f) Southern Apennines; g) Calabrian Area; h) Sicily and background sources.

decay. In Fig. 9c, the sources of the Northern Apennines are represented: the dispersion of the curves is significant (about 3 degrees) even if they refer to data sets with about the same number of observations; worthy of mention is the fact that many authors (e.g. Frepoli and Amato, 1998) recognise different geodynamic contexts, when going from the Tyrrhenian toward the Adriatic Sea, passing from distensive to compressive conditions. Attenuations of SZs 31, 41, and 42 (Fig. 9c and d) are alike, and can tentatively be ascribed to similar crustal properties (see Scandone, 1997). The few observations may be responsible for the behaviour of some sources (e.g. 43, 44, 54 and 57) experiencing moderate earthquakes (I_o < VIII); a similar decay is also obtained with more documented data sets (e.g. SZ 45). In Fig. 9e, SZs 46 and 51 exhibit similar shapes, with quite a sharp attenuation; the other curves group together at an 100-150 km distance. In Fig. 9f the SZs 56 and 57 show a "volcanic" behaviour. The peculiarity of this figure and the one after (Fig. 9g) is the very similar decay of intensity in the near field; nearly all the curves start at about 10 km *(D_o)*, and this is probably an effect of the source finiteness of high intensity earthquakes experienced in the Southern Apennines; in the far-field, the mean attenuation curve is more cautious than the Grandori ones. Fig. 9h is an example of the attenuation variability met; SZ 73 corresponds to the Mt. Etna volcano, a group of similar curves represents the Calabrian-Sicilian sources, with the anomalous behaviour of SZ 79. Finally SZ 80 and the background source in the Po Plain (marked with bkb, see Fig. 4) are expected to influence the computed intensities even at large distances.

6. Conclusions

I used macroseismic data sets of Italian earthquakes to calibrate coefficients of macroseismic attenuation relationships for seismic hazard assessment purposes; about one hundred events were treated, and 59 retained, to characterise the propagation properties of macroseismic intensity (Table 1); each curve is meant to represent the behaviour of one seismogenic source (Fig. 4), as it derives from the most dangerous, or the best documented earthquake of the SZ. Clearly, this choice is nearer to the observed data rather than the use of a mean relation for the whole territory, but not so complex as a realistic modelling of the source/path/site could be. The proposed methodology is a first step toward attenuation determinism since the representative earthquakes can be considered selected design earthquakes. The model proposed from Grandori et al. (1987) defines a finite circular source, represented by the coefficient D_o; the methodology to compute the unknown coefficients is just touched here (Figs. 1 and 2), as it has been presented elsewhere (Peruzza, 1995; 1996a). This study does not want to explore the possible geodynamic implications, or suggest physical properties of the source: it accepts that a macroseismic data set is the sum of many factors that we may not be able to isolate: source, path and site effects, the cumulative damage due to earthquake sequences, the influence of insufficient spatial sampling, and even the hand of different data set compilers; these are all topics that deserve further investigation. On the other hand, it meets the need for formal procedures to obtain attenuation coefficients, in order to reproduce the effects on the most dangerous part of the field.

The curves obtained (Fig. 9) show a wide variability, thus justifying their utilisation. In some cases the curves are similar, but refer to quite different Grandori coefficients (non-linearity of the function); sometimes similar coefficients give different values of intensity decay (function unstable): this is an important warning, as at times attenuation characteristics are mapped according to the values of the attenuation coefficients; this does not hold in absolute for a Grandori-like model.

The evaluation of attenuation reliability is a not trivial topic. The statistical errors of the curve fitting (Fig. 2) are not significant, because the use of fractile distances artificially reduces the variance of observed data. Mean residuals on the observations indicate that usually the uncertainty is lower than one degree of intensity, even if strong fluctuations are detected (Fig. 6). Even grouping all the residuals we are not able to recognise the superiority of the multiple Grandori parametrization with respect to one single mean relationship (Fig. 7); if residuals are grouped according to intensity classes (Fig. 8), it is evident that the mean CRAM model cannot properly represent the near-field conditions; the variance of the residuals is usually similar in both the approaches (i.e. using a multiple Grandori model, or a single CRAM model, see Tab. 3) but the mean values remain close to zero only using multiple relationships; the shift of the CRAM mean residuals in the highest intensity classes makes the underestimation of the strongest damages significant.

The multiple law attenuation coefficients were applied to the seismicity rates of seismogenic sources, in the Cornell-type probabilistic seismic hazard assessment of Italy (Slejko et al., 1998) performed by the GNDT. In addition, the relationships were deterministically applied to all the earthquakes falling inside the same source, to evaluate the maximum computed intensity at the site. This information has been used to fill the gaps in observations during the compilation of the map of the maximum observed intensity (Molin et al., 1997).

Acknowledgements. This research was conducted in the framework of the GNDT activities, and benefits from the work of all members of the "Seismicity" working group, among whom special thanks are due to the coordinator, Massimiliano Stucchi. Fruitful discussions were held with Dario Slejko, Paolo Scandone, and David Perkins; the paper remained unpublished until Roger Musson motivated me to finish it. They are all thanked for their support.

References

Ambraseys N. N.; 1985: *Intensity-attenuation and magnitude-intensity relationships for northwest European earthquakes.* Earth. Engin. Struct. Dyn., **13**, 733-778.

Bakun W. H. and Wentworth C. M.; 1997: *Estimating earthquake location and magnitude from seismic intensity data*. Bull. Seism. Soc. Am., **87**, 1502-1521.

Barbano M. S.; 1985: *The Val di Noto earthquake of January 11, 1693.* In: Postpischl D. (ed), Atlas of isoseismal maps of Italian earthquakes. PFG-CNR, Quaderni Ricerca Scientifica, 114, 2A, Bologna, pp. 48-49.

Bender B. and Perkins D. M.;1987: *Seisrisk III: a computer program for seismic hazard estimation*. U.S. Geological Survey Bulletin, 1772, 48 pp.

Berardi R., Magri L., Mucciarelli M., Petrungaro C. and Zanetti L.; 1994: *Mappe di sismicità per l'area italiana*. ENEL, Roma, 60 pp.

Boschi E., Ferrari G., Gasperini P., Guidoboni E., Smriglio G. and Valensise G. (eds); 1995: *Catalogo dei forti terremoti in Italia dal 461 a.C. al 1980.* Bologna, 970 pp.

Boschi E., Guidoboni E., Ferrari G., Valensise G. and Gasperini P. (eds); 1997: *Catalogo dei forti terremoti in Italia dal*

461 a.C. al 1990. Bologna, 644 pp.

Camassi R. and Stucchi M.; 1996: *NT4.1 un catalogo parametrico di terremoti di area italiana al di sopra della soglia del danno.* CNR GNDT, Milano, 86 pp., and http://emidius.itim.mi.cnr.it/NT.html.

Campbell K. W.; 1985: *Strong-motion attenuation relations: a ten-year perspective*. Earthquake Spectra, **1**, 759-804.

Cancani A.; 1904: *Sur l'empoi d'une échelle sismique des intensités, empirique et absolute.* Verhandl. d. zweiten internat. seism. Konferenz, Leipzig, 281-283.

Cella F., Zonno G. and Meroni F.; 1996: *Parameters estimation of intensity decay relationships.* Annali di Geofisica, **39**, 1095-1113.

Console R. and Gasparini C.; 1977: *Le scale macrosismiche.* Oss. Geofisico Centrale Monte Porzio Catone, Monografia n. 7, Ist. Naz. Geofisica, Roma, 21 pp.

Cornell C. A.; 1968: *Engineering seismic risk analysis*. Bull. Seism. Soc. Am., **58**, 1583-1606.

Corsanego A., Faccioli E., Gavarini C., Scandone P., Slejko D. and Stucchi M. (eds); 1997: *L'attività del GNDT nel triennio 1993 - 1995*. CNR - GNDT, Roma, 248 pp.

Frepoli A. and Amato A.; 1997: *Contemporaneous extension and compression in the Northern Apennines from earthquake fault-plane solutions.* Geophys. J. Int., **129**, 368-388.

Grandori G., Perotti F. and Tagliani A.; 1987: *On the Attenuation of Macroseismic Intensity with Epicentral Distance*. In: Cakmak A. S. (ed), Ground Motion and Engineering Seismology, Developments in Geotechnical Engineering, 44, Elsevier, Amsterdam, pp. 581-594.

Grandori G., Drei A., Garavaglia E. and Molina C.; 1988: *A new attenuation law of macroseismic intensity*. Ninth World Conf. Earth. Eng., Tokyo, A03-01.

Grunthal G. (ed); 1993: *European Macroseismic Scale 1992 (up-dated MSK-Scale)*. Conseil de l'Europe, Cahiers du Centre Europeen de Geodynamique et de Seismologie, vol.7, Luxembourg, 79 pp.

Magri M., Mucciarelli M., and Albarello D.; 1994: *Estimates of site seismicity rates using ill-defined macroseismic data*. Pageoph, **143**, 617-632.

Molin D., Stucchi M. and Valensise G.; 1997: *Massime intensità macrosismiche osservate nei comuni italiani.* GNDT - ING - SSN, Milano Roma, 203 pp. and http://emidius.itim.mi.cnr.it/NT.html.

Monachesi G. and Stucchi M; 1997: *DOM4.1, un database di osservazioni macrosismiche di terremoti di area italiana al di sopra della soglia di danno*. http://emidius.itim.mi.cnr.it/DOM/home.html.

Musson R.; 1998: *Report on the activities of WG Macroseismology at the XXVI ESC General Assembly*. http://www.gsrg.nmh.ac.uk/~phoh/WG_report_TelAviv.htm.

Peruzza L.; 1995: *Macroseismic intensity versus distance: constraints to the attenuation model.* In: Cakmak A. S. and Brebbia C. A. (eds): Soil Dynamics and Earthquake Engineering VII, Comp. Mech. Publ., Southampton, pp. 215 - 222.

Peruzza L.; 1996a: *Attenuating intensities.* Annali di Geofisica, **39**, 1079-1093.

Peruzza L. (eds); 1996b: *Modalità di attenuazione dell'intensità macrosismica*. Rapporto Sintetico per il GdL "Rischio Sismico", OGS, Trieste, 8 pp. and http://emidius.itim.mi.cnr.it/NT.html.

Peruzza L. and Mucciarelli M.; 1997: *L'attenuazione dell'intensità macrosismica.* In: Corsanego A., Faccioli E., Gavarini C., Scandone P., Slejko D. and Stucchi M. (a cura di); L'attività del GNDT nel triennio 1993 - 1995. CNR - GNDT, Roma, pp. 43 - 50.

Postpischl D., Branno A., Esposito E. G. I., Ferrari G., Marturano A., Porfido S., Rinaldis V. and Stucchi M.; 1985: *The Irpinia earthquake of November 23, 1980.* In: Postpischl D. (ed), Atlas of isoseismal maps of Italian earthquakes, Quaderni della Ricerca Scientifica, 114, 2A, Roma, pp.52-59.

Scandone P.; 1997: *Linea di ricerca 2 "Sismotettonica"*. In: Corsanego A., Faccioli E., Gavarini C., Scandone P., Slejko D. and Stucchi M. (eds), L'attività del GNDT nel triennio 1993 - 1995, CNR - GNDT, Roma, pp. 67-96.

Slejko D., Peruzza L. and Rebez A.; 1998: *Seismic hazard maps of Italy*. Annali di Geofisica, **41/2**, 183-214.

Stucchi M. (coord); 1997: *Review of Historical Seismicity in Europe (RISHE).* EC Project at: http://emidius.irrs.mi.cnr.it/RHISE/home.html.